07;08

Features of the radiative properties of quantum-size particles of narrow-gap semiconductors

© N.D. Zhukov, S.A. Sergeev, A.A. Hazanov, I.T. Yagudin

Saratov National Research State University, Saratov, Russia
E-mail: ndzhukov@rambler.ru

Received June 17, 2021
Revised July 30, 2021
Accepted August 6, 2021

For colloidal quantum-size particles (QP) of narrow-gap semiconductors, in contrast to quantum dots of wide-gap CdSe, in QP-PbS there take place an anomalous temperature dependence of the photoluminescence intensity. Also, in the planar microstructure containing QP-InSb, long-wavelength radiation (more than $3\,\mu$m) and photoconductivity (over $20\,\mu$m) was observed. Under certain conditions, the radiation intensity and photoconductivity demonstrate a resonance maximum. The effects were explained in the model of a one-dimensional quantum oscillator, which energy substantially depends on the effective mass of its quasi-free electron. This leads to competition between the manifestations of long-wave radiation and photoluminescence, and hence, to the anomalous temperature dependence of photoluminescence. It is assumed that QP-InSb in a planar microstructure can be sources and receivers of terahertz radiation, which properties depend on the crystal structure of quantum-sized particles determined by the parameters of their synthesis.

Keywords: quantum-dimensional particle, quantum dot, narrow-gap semiconductor, effective mass, Brillouin zone, dimensional quantization, quantum oscillator, photoluminescence, long-wavelength radiation.

DOI: 10.21883/TPL.2022.14.55123.18927

A considerable number of studies into colloidal quantum dots (QDs) focused primarily on relatively wide-gap semiconductors (cadmium chalcogenides) have been published in recent years [1]. The key modern trend is the synthesis and examination of nanoscale objects of various shape: polygonal and large QDs, nanowires, nanoplatelets, nanorolls, etc. [2]. Earlier research into QDs and their applications was focused mostly on their emission (photoluminescence). The variety of shapes and sizes creates opportunities for novel applications in, e.g., micro- and nanoelectronics [3].

A quantum dot is a zero-dimensional physical object. Colloidal QDs are actually three-dimensional objects, quantum-dimensional particles (QPs). The quantization dimensions in them are defined by the quantum model parameters (specifically, by de Broglie wavelength $\Lambda = h(2m\mathscr{E})^{-1/2}$ for an electron in a semiconductor, where h is the Planck constant, m is the effective mass of an electron, and $\mathscr{E}$ is its kinetic energy). QP dimensions a_i should not exceed Λ.

A quantum-dimensional particle differs from a QD in that its crystal structure and anisotropy of properties are of fundamental importance. Narrow-gap semiconductors, which feature high values of dimensional quantization parameters owing to the specifics of their band structure, are of particular interest in this regard. For example, the quantization dimension may reach 60 nm [4] for InSb, which features an extremely small effective electron mass m ($m \sim 0.014m_0$, m_0 is the „rest“ mass of an electron), and 25 nm [5] for PbS ($m/m_0 \sim 0.07$). In view of this, the properties of QPs (specifically, emissive characteristics) should differ from those of QDs. While photoluminescence of QDs of relatively wide-gap semiconductors, such as CdSe, is governed by the exciton model and has high intensity levels, narrow-gap semiconductors (e.g., InSb and PbS) feature a much weaker photoluminescence effect that is sustained by other mechanisms [6].

The aim of the present study is to investigate the specifics of emissive properties of the most thoroughly studied quantum-dimensional particles of narrow-gap semiconductors: QP-PbS and QP-InSb. QPs were produced by colloidal synthesis [7] and examined by photoluminescence spectroscopy [6], transmission electron microscopy (TEM) [8], and CVC (current–voltage curve) analysis [9].

The results of TEM studies performed with a Libra-120 (Carl Zeiss, Germany) microscope revealed that QP nanocrystals have polygonally faceted morphologies (Fig. 1, *a*) matching the crystal system of semiconductors. This should translate into typical crystalline properties, such as anisotropy, marked influence of the band structure parameters, quantum-dimensional effects, etc.

The size of nanoparticles was determined by analyzing random samples from TEM images under high magnification on a computer screen in rows of 100 consecutive particles. It was found that the distribution for slow (quasi-equilibrium) crystallization had two maxima (Fig. 1, *b*, curve *1*). This may be attributed to the non-isotropic growth of crystals governed by the anisotropy of thermodynamic properties of the lattice.

The spectral photoluminescence curve for QP-PbS with two maxima of the size distribution also had two maxima (Fig. 1, *b*, curve *3*). The corresponding temperature dependence of the emission intensity was anomalous in

nature (Fig. 2). The photoluminescence data for QP-InSb were not analyzed, since the emission intensity was very low.

According to the theory of a 3D quantum-dimensional particle, the energy spectrum of allowed electron states in the model of a deep extended potential well and in the effective mass approximation is determined by solving the Schrödinger equation and is presented as [10]

$$\mathscr{E}_{glp} = h^2(8m)^{-1}(g^2a_x^{-2} + l^2a_y^{-2} + p^2a_z^{-2}),$$

where $g, l, p = 1,\ 2,\ 3,\ldots$ are quantum numbers; a_x, a_y, and a_z are the x-, y-, and z- axis dimensions of a quantum cell, respectively. In the case of cubic symmetry ($a_x = a_y = a_z = a$),

$$\mathscr{E}_{glp} = 3h^2(8ma^2)^{-1}(g^2 + l^2 + p^2).$$

$\mathscr{E}_1 = 3h^2(8ma^2)^{-1} \approx (m/m_0)^{-1}a^{-2}$ ($\mathscr{E}$ — [eV], a — [nm]) for the non-excited energy level. The spectral dependences of photoluminescence (Fig. 1, *b*, curve *2*) calculated in accordance with this formula match closely in maxima at $m/m_0 \sim 0.07$ for the first maximum and $m/m_0 \sim 0.1$ for the second one. With the anisotropy of properties taken into account, these m/m_0 values match the known values for film and bulk lead sulfide samples [5,11].

In the process of photoluminescence, electrons are excited by high-energy quanta from the valence band to the conduction band, thermalize, interact with holes (e.g., by forming excitons), and recombine to emit photons. Owing to high mobilities of electrons (low m/m_0 values), the probability of exciton formation in narrow-gap semiconductors at room temperature is negligible. Other excitation mechanisms are needed in this case. We used the emission–injection mechanism in a multigrain microstructure that was discussed in detail in our earlier studies [12,13]. Subjected to the influence of the field applied to a microstructure, an excited electron is emitted from a certain QP into a nanogap and is then injected into a neighboring QP, where it undergoes a transition to the non-excited state. We assume that energy in the form of quanta $h\nu = \mathscr{E}_i \approx (m/m_0)^{-1}a_i^{-2}$ should be radiated in the process. For example, the emission wavelength at $a = 5$ nm should be $\sim 3\,\mu$m for QP-PbS and $\sim 20\,\mu$m for QP-InSb. It was of interest to observe long-wavelength (infrared and terahertz) emission in this context. Relatively large QP-InSb, which were synthesized and examined in our study [14], were used for the purpose.

Measurements of the spectrum and intensity of long-wavelength (infrared and terahertz) emission are rather hard to perform. The science and technology of this issue have been discussed extensively (see [15]). The most difficult part is the detection of weak signals, which is exactly what we have to deal with here. Photodetectors have very complex designs and are not readily available. The lack of emission and photoconductivity at shorter wavelengths (up to 3 and 20 μm, respectively) was established reliably using a specialized spectroscopic system comprised of an MDR-41 monochromator with interchangeable diffraction gratings and a proper set of sources and photodetectors [16].

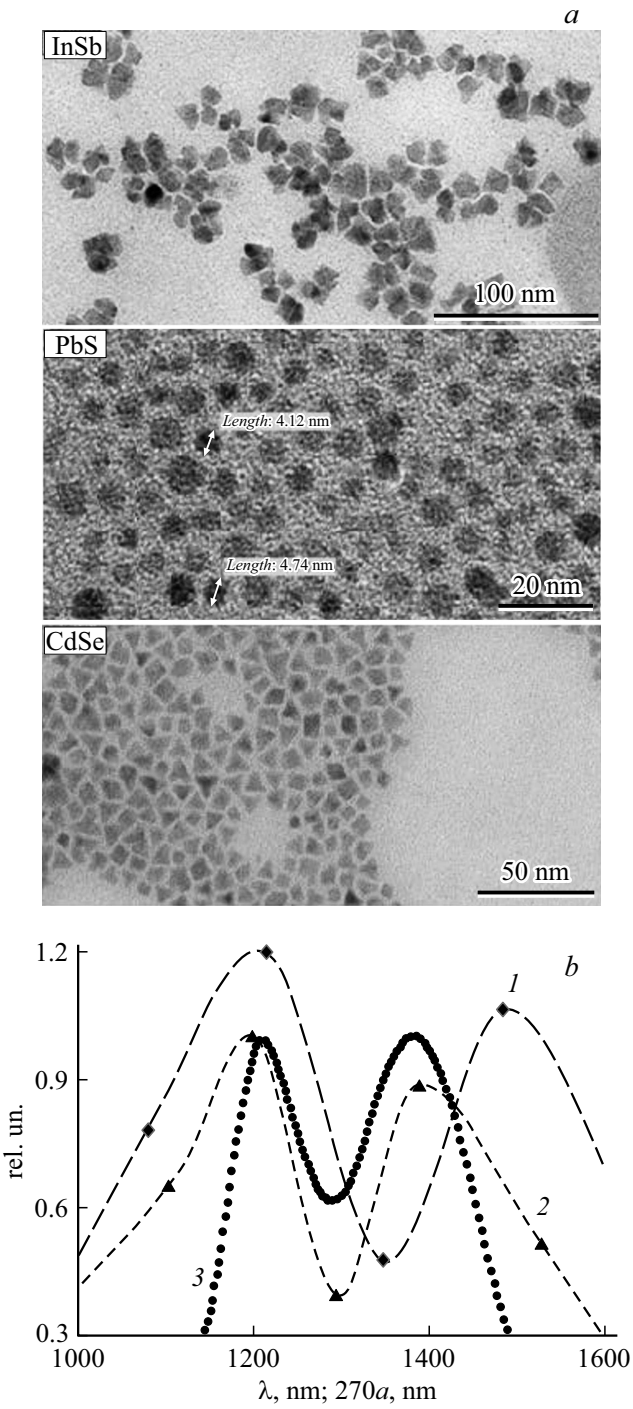

Figure 1. *a* — Fragments of TEM images of QP-InSb, QP-PbS, and QD-CdSe from [8] (for comparison); *b* — experimental (*1*) particle size distribution for QP-PbS ($270a$ on the abscissa axis) and photoluminescence spectra (*2, 3*) for QP-PbS (λ on the abscissa axis).

When the proposed microstructure emits radiation, it, in accordance with the reciprocity principle, should also react

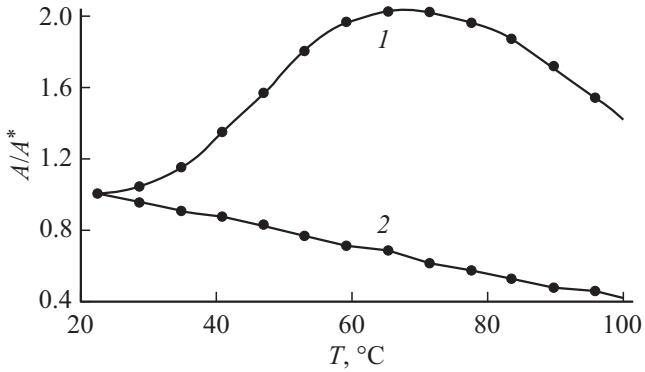

Figure 2. Temperature dependences of the ratio of photoluminescence intensity A at the spectral maximum to intensity A^* at a temperature of 22°C: *1* — for QP-PbS (anomalous), *2* — for QD-CdSe (normal).

to this radiation (i.e., serve as a photodetector). We carried out the experiments needed to verify this.

One of two identical QP-InSb samples, which were fabricated in accordance with the procedure detailed in [13], served as an emitter, and the other was a detector. Supply voltage $V_=$ was applied to the emitter, and CVCs were measured at the detector using the technique outlined in [13]. The lack of an unwanted (electric and capacitive) interaction between samples was verified so as to guarantee that one sample could influence the other only via electromagnetic radiation. The influence of thermal radiation due to heating of the source was estimated and was found to be negligible.

The CVC measurement results are presented in Fig. 3. The detector current increased considerably as emitter supply voltage $V_=$ grew from 30 to 100 V. At $V_= = 60$ V, a current spike was observed (Fig. 3, *a*). The examination of CVCs plotted in different coordinates (Fig. 3, *b*) were performed with account for the single-electron transport model [10] and demonstrated that the mechanism limiting this transport in the QP-InSb detector structure at $V_=$ = 30 and 100 V is the current limited by charge localized in QPs, and emission from QPs acts as such a mechanism at $V_= = 60$ V. This suggests that the process of transport of electrons (injected and thermalized in QPs) is limited in the detector structure under a relatively mild influence, while the process of emission into intergrain nanogaps is limited under a stronger influence.

QPs with a perfect crystal structure are specific in that both the energy and momentum of an electron are quantized; i.e., its motion is governed by the properties of the Brillouin zone. One may assume in this case that the resonance motion of an electron in a QP is linear and apply the model of a one-dimensional harmonic oscillator [17].

We attribute the sharp detector current rise at voltage $V_= = 60$ V (Fig. 3, *a*) to an increase in the emission intensity due to a probable energy transition of the quantum oscillator to the first resonance level ($n = 1$). According to the formula for quantum oscillator energy $\mathscr{E} = \mathscr{E}_0(n + 1/2)$ [17], the emission intensity (in the present case, the detector current) should increase by a factor of approximately 1.5, which is exactly what is observed in Fig. 3, *a*: the ratio of currents for $V_= = 60$ and 30 V is $\sim 5:3$.

The fabricated and tested structures with QD-CdSe and QP-PbS did not manifest the discussed effect of long-wave emission and photoconductivity.

Thus, if a quantum-dimensional particle is represented as a quantum oscillator, the difference in effective mass m/m_0, which is the key property of electrons characterizing their mobility, explains why QP-InSb, in contrast to QD-CdSe, feature long-wave emission and lack photoluminescence: the value of m/m_0 for QP-InSb is the lowest (~ 0.014), while m/m_0 for QD-CdSe is ~ 0.15. Both effects (long-wave emission and photoluminescence) are weak in QP-PbS with an intermediate value of $m/m_0 \sim 0.07$, although photoluminescence is somewhat more pronounced. The anomalous temperature dependence of photoluminescence

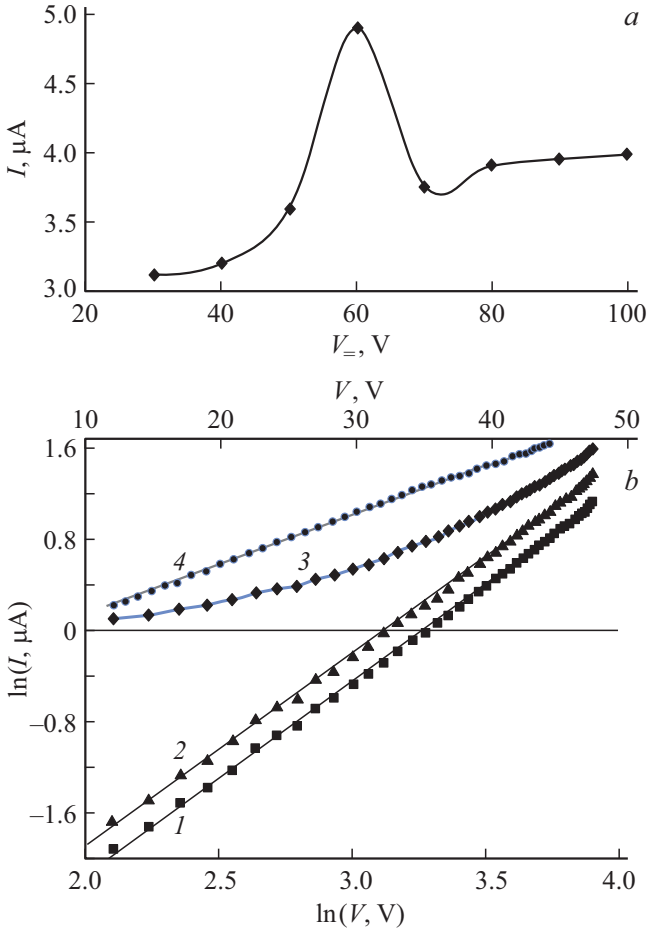

Figure 3. *a* — Dependence of the detector current at $V = 50$ V on voltage $V_=$ at the emitter; *b* — detector CVC at different values of $V_=$ (linear approximation parameters are given in brackets) in $\ln I \sim \ln V$ coordinates: *1* — $V_= = 30$ V ($y = 1.693x - 5.513$, $R^2 = 0.997$), *2* — $V_= = 100$ V ($y = 1.693x - 5.265$, $R^2 = 0.997$), *3* — $V_= = 60$ V; and in $\ln I \sim V$ coordinates: *4* — $V_= = 60$ V ($y = 0.036x - 0.181$, $R^2 = 0.999$).

is assumed to be shaped by the competing influences of quantum-dimensional and exciton mechanisms. In future studies, we plan to optimize the QP structure and perform spectral measurements directly in the terahertz range in order to enhance long-wave emission and detect it.

Acknowledgments

The authors wish to thank A.G. Rokakh for helpful advice.

Funding

This study was supported financially by the Russian Foundation for Basic Research as part of research project 20-07-00603-a.

Conflict of interest

The authors declare that they have no conflict of interest.

References

[1] M. Alizadeh-Ghodsi, M. Pourhassan-Moghaddam, A. Zavari-Nematabad, B. Walker, N. Annabi, A. Akbarzadeh, Part. Part. Syst. Charact., **36** (2), 180030 (2019). DOI: 10.1002/ppsc.201800302
[2] D. Porotnikov, M. Zamkov, J. Phys. Chem. C, **124** (40), 21895 (2020). DOI: 10.1021/acs.jpcc.0c06868
[3] N. Sitapure, N. Varadan, S. Malani, P. Goswami, M.A.K. Kerawalla, Int. J. Adv. Res. Eng. Appl. Sci., **5** (6), 29 (2016). https://garph.co.uk/IJAREAS/June2016/3.pdf
[4] S. Tamang, K. Kim, H. Choi, Y. Kim, S. Jeong, Dalton Trans., **44** (38), 16923 (2015). DOI: 10.1039/c5dt02181b
[5] S.I. Sadovnikov, N.S. Kozhevnikova, A.A. Rempel, Semiconductors, **44** (10), 1349 (2010). http://journals.ioffe.ru/articles/viewPDF/7252
[6] N.D. Zhukov, D.V. Kryl'skiy, M.I. Shishkin, A.A. Khazanov, Semiconductors, **53** (8), 1082 (2019). DOI: 10.21883/FTP.2019.08.48002.9037
[7] D.V. Krylsky, N.D. Zhukov, Tech. Phys. Lett., **45** (8), 801 (2019). DOI: 10.21883/PJTF.2019.16.48147.17665
[8] A.V. Katsaba, V.V. Fedyanin, S.A. Ambrozevich, A.G. Vitukhnovsky, A.N. Lobanov, A.S. Selyukov, R.B. Vasiliev, I.G. Samatov, P.N. Brunkov, Semiconductors, **47** (10), 1328 (2013). https://doi.org/10.1134/S1063782613100138
[9] N.D. Zhukov, M.V. Gavrikov, D.V. Kryl'skii, Tech. Phys. Lett., **46** (9), 881 (2020). DOI: 10.21883/PJTF.2020.17.49895.18355
[10] V.P. Dragunov, I.G. Neizvestnyi, V.A. Gridchin, *Osnovy nanoelektroniki* (Logos, M., 2006) (in Russian).
[11] E.V. Maraeva, *Poluchenie i issledovanie nanostrukturirovannykh polikristallicheskikh sloev i sistem s kvantovymi tochkami na osnove khal'kogenidov svintsa*, Candidate's Dissertation in Mathematics and Physics (S.-Peterb. Gos. Elektrotekh. Univ. „LETI,"SPb., 2014) (in Russian).
[12] N.D. Zhukov, V.F. Kabanov, A.I. Mihaylov, D.S. Mosiyash, A.A. Hazanov, M.I. Shishkin, Semiconductors, **52** (1), 78 (2018). DOI: 10.1134/S1063782618010256
[13] N.D. Zhukov, I.T. Yagudin, N.P. Aban'shin, D.S. Mosiyash, Tech. Phys. Lett., **46** (11), 1088 (2020). DOI: 10.21883/PJTF.2020.21.50196.18392
[14] D.V. Krylsky, N.D. Zhukov, Tech. Phys. Lett., **46** (9), 901 (2020). DOI: 10.21883/PJTF.2020.18.49995.18358
[15] I.S. Gibin, P.E. Kotlyar, Usp. Prikl. Fiz., **6** (2), 117 (2018) (in Russian). http://advance.orion-ir.ru/UPF-18/2/UPF-6-2-117.pdf
[16] N.D. Zhukov, M.I. Shishkin, A.G. Rokakh, Tech. Phys. Lett., **44** (4), 362 (2018). DOI: 10.1134/S1063785018040284
[17] L.K. Martinson, E.V. Smirnov. Kvantovaya fizika [Electronic resource] (in Russian). URL: http://fn.bmstu.ru/data-physics/library/physbook/tom5/ch4/texthtml/ch4_5.htm